Available online at www.sciencedirect.com
SCIENCE DIRECT
Biochimica et Biophysica Acta 1715 (2005) 71 – 80
BIOCHIMICA ET BIOPHYSICA ACTA
BBA
http://www.elsevier.com/locate/bba

Temperature dependence of the Langmuir monolayer packing of mycolic acids from *Mycobacterium tuberculosis*

Masumi Villeneuve[a,*], Mizuo Kawai[a], Hideki Kanashima[a], Motoko Watanabe[b], David E. Minnikin[c], Hiroo Nakahara[a]

[a]*Department of Chemistry, Faculty of Science, Saitama University 255 Shimo-okubo, Saitama 338-8570, Japan*
[b]*School of Pharmacy, Tokyo College of Pharmacy and Life Science, Horinouchi, Hachioji, Tokyo 192-0329, Japan*
[c]*School of Biosciences, The University of Birmingham, Edgbaston, Birmingham B15 2TT, UK*

Received 7 February 2005; received in revised form 23 June 2005; accepted 19 July 2005
Available online 9 August 2005

Abstract

Phase diagrams of the Langmuir monolayer of dicyclopropyl alpha mycolic acid (α-MA), cyclopropyl methoxy mycolic acid (MeO-MA), and cyclopropyl ketomycolic acids (Keto-MA) from *Mycobacterium tuberculosis* were obtained by thermodynamic analysis of the surface pressure (π) vs. average molecular area (A) isotherms at temperatures in the range of 10–46 °C. The Langmuir monolayers of MAs were shown to exhibit various phases depending on the temperature (T) and the π values. In the Langmuir monolayer of Keto-MA, the carbonyl group in the meromycolate chain apparently touches the water surface to give the molecule a W-shape in all the temperatures and surface pressures studied. Keto-MA formed a rigid solid condensed film, with four hydrocarbon chains packing together, not observed in the others. In contrast, the monolayer films of α-and MeO-MAs having no such highly hydrophilic intra-chain groups in the meromycolate chain were mostly in liquid condensed phase. This novel insight into the packing of mycolic acids opens up new avenues for the study of the role of mycolic acids in the mycobacterial cell envelopes and pathogenic processes.

Keywords: Mycolic acid; *Mycobacterium tuberculosis*; Langmuir monolayer; Thermodynamics; Phase diagram; Fatty acid conformation

1. Introduction

Mycolic acids (MAs) are high-molecular-weight 2-alkyl, 3-hydroxy fatty acids, abundantly present in the mycobacterial cell envelope (about 30% of the dry weight of *Mycobacterium tuberculosis* (*M. tb* [1]), mostly as bound esters of arabinogalactan, and some as extractable lipids, mainly as trehalose 6,6-dimycolate (TDM) (cord factor) [2,3]. MA consists of two characteristic parts, i.e., a saturated carboxylic acid part and a long fatty alcohol part called a meromycolate chain, as shown in Table 1. The meromycolate chain from pathogenic mycobacteria normally has two intra-chain groups that vary in the type, stereochemistry and spacing in between. On the basis of the nature of the functional groups in the meromycolate chains, MAs from *M. tb* are categorized into three major groups: α-MA with no oxygen-containing intra-chain groups, methoxy-MA (MeO-MA) in which the distal group has a methoxy group and Keto-MA in which the distal group has a carbonyl group. MeO-MA and Keto-MA have methyl branches next to the oxygenated functional groups and natural mixtures have both *cis*- and *trans*-cyclopropane rings, the latter having an adjacent methyl group (Table 1). The nature and the locations of the groups in the meromycolate chains of MAs from representative mycobacteria have been studied by extensive NMR and mass spectroscopic analyses by Watanabe et al. [4,5].

According to structural models of mycobacterial cell envelope proposed by Minnikin [6,7] and Rastogi [8], MA chains are arranged in parallel and essentially perpendicular to the plane of the cell envelope and are considered to provide the cells with a special permeability barrier possibly responsible for various physiological and pathogenic fea-

* Corresponding author.
E-mail address: villeneuve@chem.saitama-u.ac.jp (M. Villeneuve).

0005-2736/$ - see front matter © 2005 Elsevier B.V. All rights reserved.
doi:10.1016/j.bbamem.2005.07.005

Table 1
Molecular structures, compositions and average molecular weights of the mycolic acids of *M. tb*

cis stereochemistry

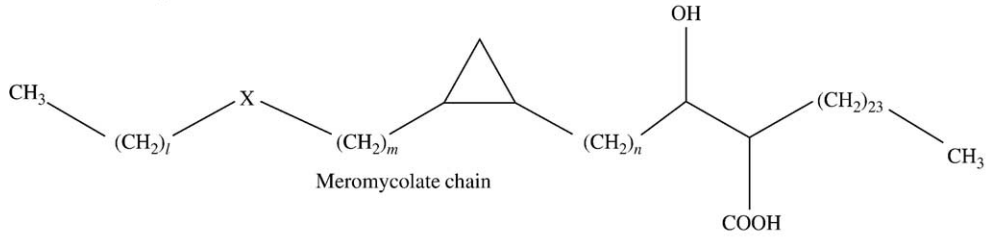

trans stereochemistry

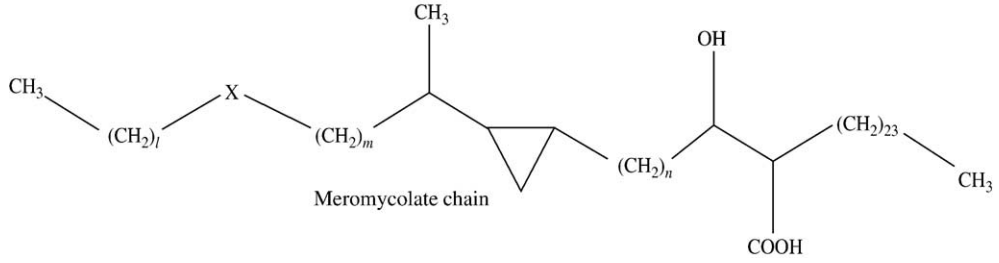

Samples	Distal group (X)	Proximal cyclopropane *cis*/*trans*, *l*-*m*-*n*	Content (%)[a]	Average MW
α-MA	*cis*-cyclopropane	*cis* 19-14-11	50[b]	1150
		cis 19-14-13	40	
MeO-MA	$CH(CH_3)$-$CH(OCH_3)$	*cis* 17-16-17	60[c]	1259
		trans 17-16-18	20	
Keto-MA	$CH(CH_3)$-CO	*cis* 17-18-15	20[d]	1267
		trans 17-18-16	70	

[a] Implied by FAB mass spectrum profile.
[b] The rest mostly $n=15$ analogue.
[c] *cis* cyclopropyl/*trans* cyclopropyl ratio (by 1H-NMR spectrum)=1:0.4. Homolgues with ±28 m/z also present as minor components.
[d] *cis* cyclopropyl/*trans* cyclopropyl ratio (by 1H-NMR spectrum)=1:3.5. Homolgues with ±28 m/z also present as minor components.

tures of mycobacterial cells as implied by earlier works [9,10]. In a mutant strain of *Mycobacterium tuberculosis* H37Rv containing 40% less cell wall linked mycolates than the wild type, the diffusion rate of glucose through the cell wall layer was shown to be quite high [9]. *Mycobacterium smegmatis* mutant that produced no mycolates but accumulated arabinogalactan-bound meromycolates was hypersensitive to hydrophobic antibiotics such as rifampicin and erythromycin [10]. Nikaido et al. have reported X-ray diffraction studies of mycobacterial envelopes free of plasma membranes, which supported the MA arrangement on the cell envelope proposed [11]. The computer simulation work by Hong and Hopfinger also supported the MA arrangement in cell envelope proposed [12].

In very early studies [13], the multi-component nature of mycolic acids was not yet known, but it was shown that the total MA formed a stable monolayer on the water surface. It was concluded that MA had extended linear structures, a feature later confirmed by structural analysis [6–8,21,22]. Both in the monolayer on the water surface and in the proposed cell envelope lipid structure models, MA is considered to take the same structural arrangement, with the hydrophilic 3-hydroxy and 2-carboxyl groups touching the hydrophilic surface and with the aliphatic chains stretching out in parallel, and normal to the hydrophilic surface. Therefore, detailed studies on the artificial MA layers on water surface should help elucidation of the roles and the nature of actual mycolate layers in the mycobacterial cell envelope.

Recently, limited Langmuir monolayer studies have been performed on a selection of MA [14–17]. Those studies reported that, in a compressed monolayer, α-mycolic acid from *Mycobacterium avium* apparently took a conformation with three parallel chains, and on further compression, an extended structure, but that the corresponding *M. tb* mycolate appeared to take an extended conformation. As regards the methoxy and keto mycolates from *M. tb*, they were reported to take triple chain folded conformations [15,17]. Regrettably, their monolayer experiments were limited at a single temperature of 25 °C, whereas temperature is one of the important factors that influence biological activities of the living cells.

In the present study, we analyzed the temperature effect on the Langmuir monolayer packing of a coherent set of all three α-MA, MeO-MA and Keto-MA from *M. tuberculosis*. This involves detailed physicochemical and thermal analysis of the Langmuir monolayers at temperatures in the range of

10–46 °C and clarification of their phase diagrams. In addition, their Langmuir–Blodgett (LB) films were studied by atomic force microscopy (AFM) and X-ray diffraction (XRD). Differential scanning calorimetry (DSC) of MA was also performed.

2. Experimental

2.1. Materials

Mycolic acids used in the present experiment were α-MA, MeO-MA and Keto-MA from *M. tb* strain Aoyama B, prepared by hydrolysis of purified relevant α-MA, MeO-MA and Keto-MA methyl esters. The procedures for separation and purification of the methyl esters including argentation thin-layer chromatography (TLC) to remove minor components with double bonds and the analytical details are described elsewhere [4,5]. Hydrolysis was performed by heating a sealed tube containing MA methyl ester (70 mg), powdered KOH (200 mg) and 2-propanol (2 ml) in an oil bath kept at 80–85 °C for 2 h with stirring. The hydrolysate was acidified with 2 N H_2SO_4 and treated with hexane, and the mycolic acid obtained was purified by TLC with hexane/AcOEt (4:1, v/v) to remove the byproduct epimer. For reference, the analytical data of the three MA samples used are given in Table 1. Distilled reagent grade chloroform (Wako chemicals) was used as the spreading media.

2.2. Measurements

Surface pressure measurement was performed by using a Lauda film balance (FW1). A Langmuir monolayer was prepared by spreading a chloroform solution of MA (1 ml, ca. 6×10^{-5} M) onto deionized distilled water (Milli-Q Plus, 18.2 MΩ cm) in the trough. The surface pressure (π) vs. average molecular area (A) isotherms were prepared by compressing the surface monolayer at a rate of 14 $Å^2$ $molecule^{-1}$ min^{-1} and by measuring the pressure with the balance. The subphase temperature was in the range of 10.0 °C to 46.0 °C as given in Fig. 1, and the accuracy was ±0.2 °C. The room temperature was thermostated at 23 ± 1 °C.

A single layered LB film, often referred to as a Z type film, was prepared by transferring a single MA monolayer on the water surface onto a mica substrate by the LB method as the substrate was being withdrawn from the trough. The surface pressure was at 25 mN m^{-1} and the temperature at 20.0 and 37.0 °C. To examine the surface profile, the surface was surveyed with an atomic force microscope (AFM, Seiko instruments SPA300) at the room temperature, in the contact mode at the spring constant of 0.06 N m^{-1} with the Si_3N_4 probe.

To determine the in-plane spacing of the two dimensional lattice of a MA film by the X-ray diffraction (XRD) method, a nineteen layered alternated Y-type LB film was prepared by the standard method, by transferring 19 monolayers onto a glass substrate at 25 mN m^{-1} and at temperatures 20.0 and 37.0 °C. The diffraction was measured at the grazing angle

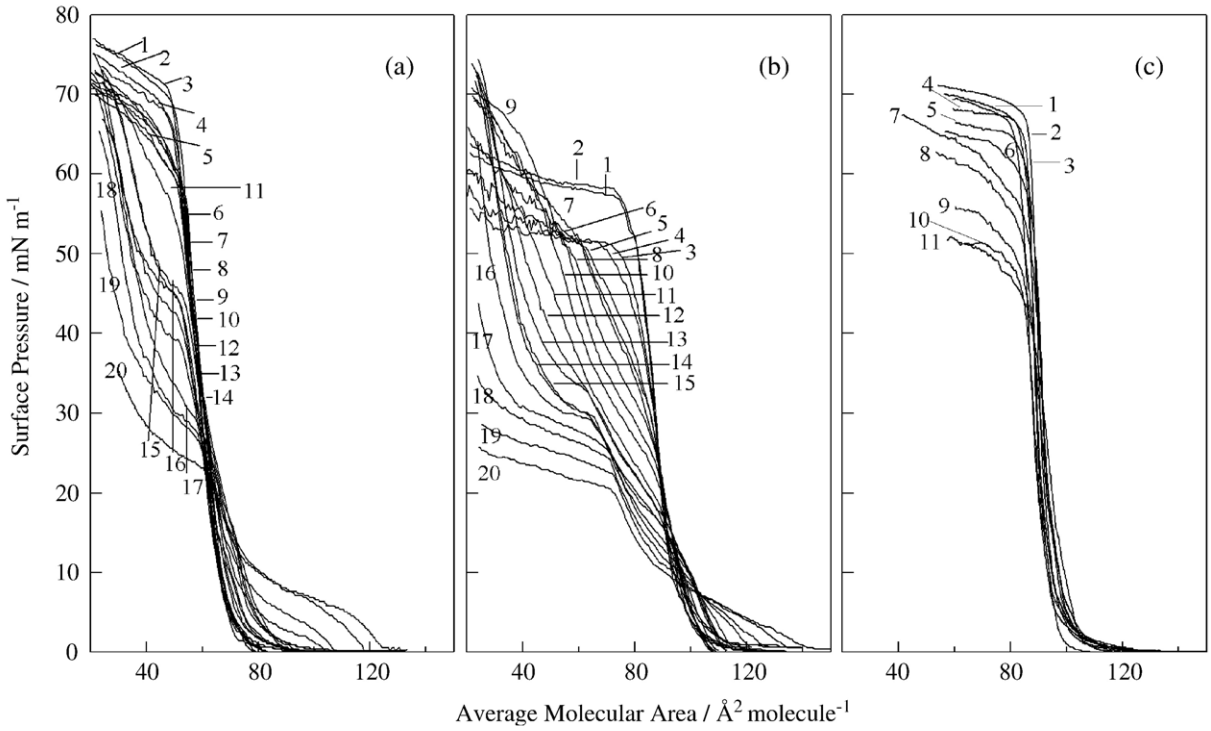

Fig. 1. Surface pressure vs. average molecular area isotherms of mycolic acids. (a) α-MA; (b) MeO-MA; (c) Keto-MA. Figures in the graphs refer to the temperatures at which the measurement was performed. In (a) and (b), 1 to 20 refer to temperatures 10, 12, 14, 16, 18, 20, 22, 24, 26, 28, 30, 32, 34, 36, 37, 38, 40, 42, 44 and 46 °C, respectively, and in (c), 1–11 refer to the temperatures 20, 22, 24, 26, 28, 30, 32, 34, 36, 37 and 40 °C, respectively.

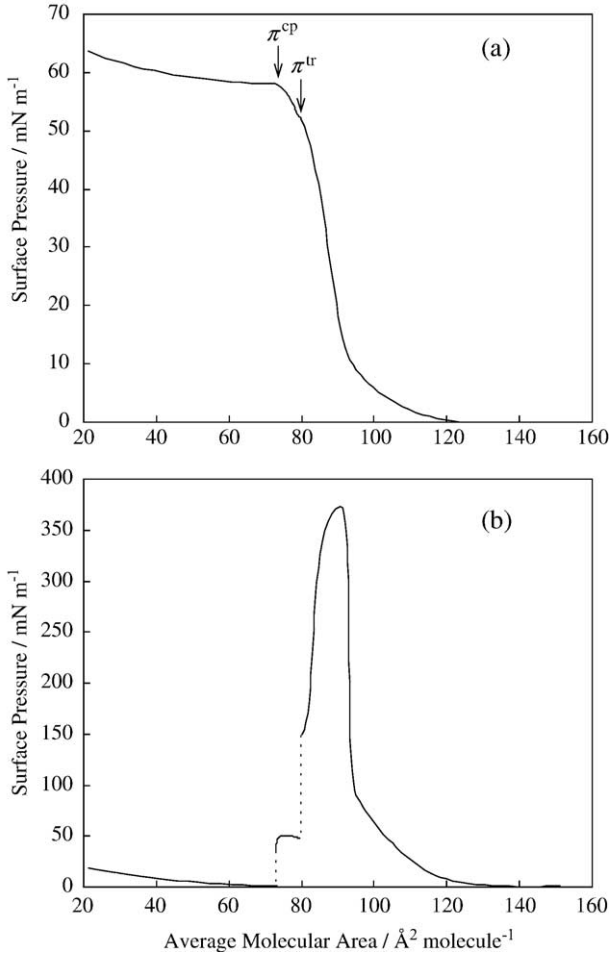

Fig. 2. (a) Surface pressure vs. average molecular area isotherm at 12 °C from Fig. 1b enlarged. π^{tr} refers to the phase transition surface pressure and π^{cp} to the film collapsing surface pressure; (b) Elasticity modulus vs. average molecular area curve obtained from (a).

of the incident X-ray at 0.2 ° by using Bruker AXS, MXP-BX (Cu-Kα radiation, 40 kV and 40 mA), which is a custom-made apparatus equipped with a horizontal sample stage. Measurement was performed at the room temperature with a scanning rate of 0.05 °/20 s. The melting temperatures were determined by the differential scanning calorimetry assay (DSC, Seik DSC 6200). The scanning rate was 1 °C/min.

3. Results and discussion

3.1. Phase diagrams

The surface pressure π vs. average molecular area A isotherms of α-MA, MeO-MA, and Keto-MA are shown in Figs. 1a–c, respectively. All the samples showed complex isotherms and gradual changes in their shapes as the temperature changed. Fig. 2 shows a representative π vs. A curve of MeO-MA isotherms at a temperature of 12 °C together with an elasticity modulus E vs. A curve to show how the phase transition and film collapse points are determined. Here, elasticity modulus E is defined by the following equation [18].

$$E = -A(\partial\pi/\partial A)_{T,p,\text{composition}}$$

In Fig. 2a, as the monolayer is compressed, the surface pressure π starts to rise at about 120 Å^2 molecule^{-1}, and increases smoothly up to $\pi = 52$ mN m^{-1} through the change in the visco-elastic nature, then the monolayer transforms to another state. Further compression finally causes the monolayer to collapse at $\pi = 57$ mN m^{-1}. The phase transition pressure π^{tr} and the film collapse pressure π^{cp} where the collapse of the films occurred, determined by calculating the slope of the curvature of each curve are marked. The E vs. A curve in Fig. 2b exhibits discontinuities at the corresponding A, which in this case are at 80.0 and 73.2 Å^2 molecule^{-1}, respectively. The value of elasticity modulus E was utilized as a criterion to characterize the state of each phase. At a film collapse point, π–A isotherm does not always have a cusp but may show a round bend. Therefore, the collapse of the insoluble monolayer was confirmed by testing the hysteresis of the π–A isotherm.

Fig. 3a demonstrates the relationship between E and the temperature of the MeO-MA films at a low ($\pi = 10$ mN m^{-1}), a medium ($\pi = 22$ mN m^{-1}) and a high surface pressures ($\pi = 44$ mN m^{-1}). At low surface pressure (Fig. 3a), when $\pi = 10$ mN m^{-1}, the E values increased to reach 150 mN m^{-1} at 20 °C, then decreased to 80 mN m^{-1} as the temperature increased to 38 °C, and, after passing a break point at around 38 °C, it further decreased to reach 20 mN m^{-1} at 46 °C. The E values of usual fatty acids in the liquid condensed (LC) state and in the liquid expanded (LE) state are known to be in the ranges of 100 to 250 mN m^{-1} and 12.5 to 50 mN m^{-1}, respectively [18]. Thus, at $\pi = 10$ mN m^{-1}, the films at temperatures from 10 to 38 °C (E values 80–140 mN m^{-1}) were assigned to be in the LC phase and the films at temperatures from 38 to 46 °C (E value 20–80 mN m^{-1}) to be in the LE phase.

At the medium surface pressure (Fig. 3a), when $\pi = 22$ mN m^{-1}, E decreased to 150 mN m^{-1} as T increased to 25 °C. The film was considered to be in the LC phase in that temperature range. Then, after a break point, as T increased, E decreased sharply to reach 50 mN m^{-1} at 30 °C, and, after a gradual decrease, at 36 °C, E showed a slow increase again to reach 60 mN m^{-1} at 46 °C. When the temperature was from 27 to 46 °C, the E value suggested that the film might be in the LE phase. However, the E values from 27 to 38 °C are lower than the E values at the corresponding temperature of the monolayer at $\pi = 10$ mN m^{-1}, which implied that in the film of this region, where T was from 27 °C to 36 °C most likely two or more phases co-existed (MP region). The E values of the LE phase at the temperature from 38 to 46 °C are slightly higher than the values shown by the LE phase film at $\pi = 10$ mN m^{-1}. Hence, this LE phase might be another LE phase with slightly higher rigidity.

At high surface pressure (Fig. 3a), when $\pi = 44$ mN m^{-1}, at temperatures 10 and 12 °C, the monolayer was apparently in the LC phase. Then, after the break point, at temperatures

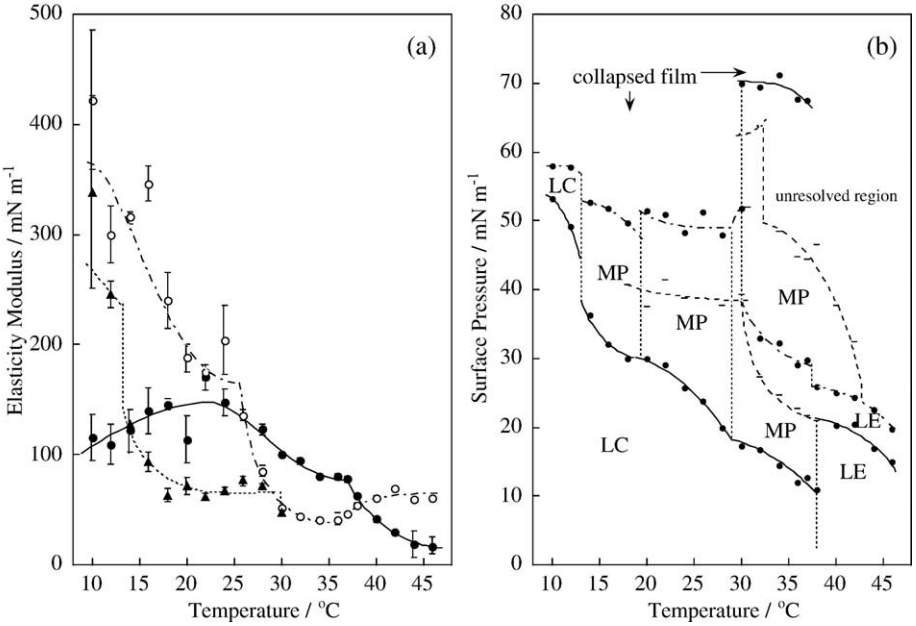

Fig. 3. (a) Elasticity modulus vs. temperature curves at constant surface pressure of MeO-MA monolayer: (— ● —) π=10 mN m^{-1}; (•—•○•—•) 22 mN m^{-1}; (- - -▲- - -) 44 mN m^{-1}. (b) Phase diagram of MeO-MA Langmuir monolayer: (—) π^{tr} vs. T curves; (•—•—•) π^{cp} vs. T curves; LC refers to the liquid condensed state, LE to the liquid expanded state and MP refers to multi-phase.

above 14 °C, E decreased to the LE phase value. However, the value was smaller than the E values of the LC phase demonstrated by the film at π=10 mN m^{-1}. Thus, it may be reasonable to conclude that the films at temperatures from 14 to 30 °C were in a MP region.

Fig. 3b is the phase diagram of the MeO-MA Langmuir monolayer isotherms shown in Fig. 1b, prepared by plotting the phase-transition pressures π^{tr} of each curve against T and the film collapse pressure π^{cp} also against T. The nature of the areas partitioned by the π^{tr}–T and the π^{cp}–T curves were assigned by the results in Fig. 3a. Fig. 3a demonstrated that the films at the low surface pressure (π=10 mN m^{-1}) were in the LC phase at temperatures from 10 to 38 °C, the films at the medium surface pressure (π=22 mN m^{-1}) were in the LC phase from 10 to 27 °C and the films at the high surface pressure (π=44 mN m^{-1}) were so from 10 to 12 °C. Then, the films at π=10 mN m^{-1} were in the LE phase at temperatures from 38 to 46 °C, and the films at π=20 mN m^{-1} were in the LE phase from 38 to 46 °C and in MP from 27 to 36 °C. The vertical dotted lines denote the temperatures where the phase transfer took place, and show the possible phases corresponding to the sections. The E vs. T at constant

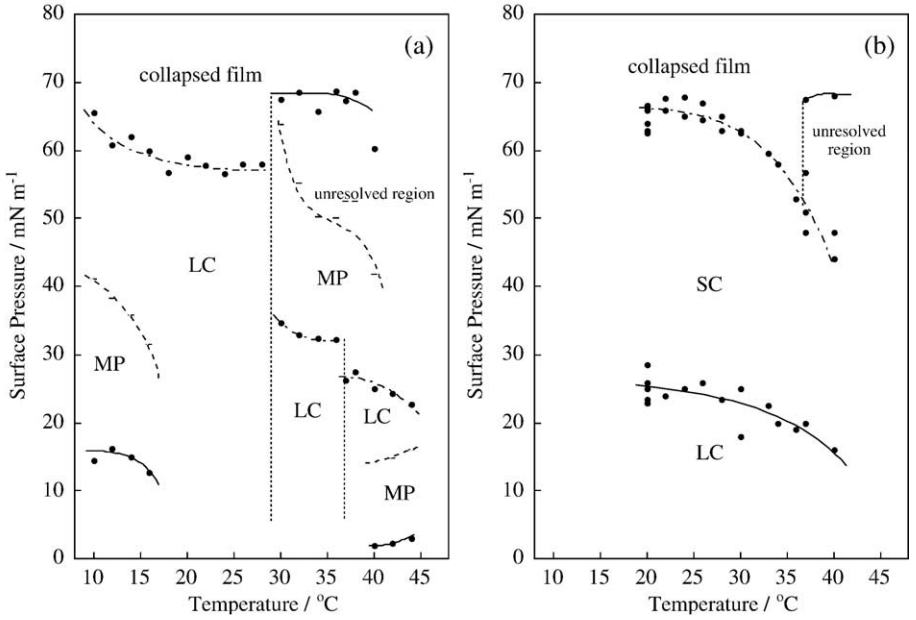

Fig. 4. Phase diagrams of Langmuir monolayers: (—) π^{tr} vs. T; (•—•—•) π^{cp} vs. T curves; SC refers to the solid condensed state. (a) α-MA; (b) Keto-MA.

Table 2
Melting temperature and enthalpy of mycolic acids of *M. tb*

Sample	Melting temperature/°C (peak top temperatures)	Enthalpy of fusion/kJ mol^{-1}
Type 1 α-MA	51.2–58.0 (54.8)	100.5
Type 1 MeO-MA	49.9–65.5 (53.0, 56.4 and 60.6)	86.4
Type 1 Keto-MA	57.8–68.5 (62.1 and 65.2)	124.5
Myristic acid	54.4	45.0
Palmitic acid	62.9	54.3

Results of only the first scans are shown.

π plot curves in Fig. 3a and A vs. T at constant π curves (not demonstrated) show discontinuities or break points at the corresponding temperatures. For example, the diagram shows that the films at the high surface pressure (π=44 mN m^{-1}) are to be at the phase boundaries at 13, 19, 29 and 30 °C. From 10 to 12 °C, the monolayer is in the LC phase, then transforms into another phase of smaller elasticity at a temperature between 12 and 14 °C then to another phase between 18 and 20 °C and yet to another phase at 30 °C.

Additionally, unidentified transitions were observed at around π=70 mN m^{-1} at temperatures above 30 °C. The mean molecular surface area at these transitions is approximately 20 Å^2 molecule^{-1}, which is too small for the area expected from the molecular structure of MeO-MA. A plausible explanation, therefore, may be that the surface monolayer forms a triple layer at the π^{cp}, which was subjected to another transition to form a multiple-layer membrane, or it may be that at 30 °C and π=32 mN m^{-1}, the solubility of the MeO-MA monolayer increases abruptly and thus the new transition means the true collapse of the monolayer.

Phase diagrams of the α-MA and Keto-MA monolayers were analogously prepared and are shown in Figs. 4a and b, respectively. As for Fig. 4a, the regions under the MP ones below T=16 °C and above 40 °C are left unspecified since the E values there were not accurate enough to discuss the nature of the phase. In the α-MA monolayer, the LC phase is more extended and the coexisting region smaller than in the case of MeO-MA monolayer. Moreover, π^{cp} at the lower temperatures is much higher than in the MeO-MA monolayer. In the Keto-MA films, along with the LC phase is observed a solid condensed (SC) phase, which is not seen in the α-MA and MeO-MA films. The E value was in the range of 1000 to 1600 mN m^{-1}, which is slightly lower than the E values known for the SC phase of usual fatty acid monolayers (1000–2000). This demonstrates that the intrachain groups in the meromycolate chain may have some effect on the E value.

The melting temperatures and the enthalpies of fusion of the bulk solid of MAs determined by DSC are summarized in Table 2. The first scanning gave two or more peaks in the thermogram, whereas the second scanning gave only one peak at a lower temperature than the lowest peak in the first scanning. An explanation may be that after the first melting followed by cooling and solidification, the components of the original solid MA sample form a eutectic mixture to give a mass of a lower melting point. The original multi-melting point mass may be regained by adding methanol to a chloroform solution of MA to slowly precipitate MA. The melting temperatures of those MAs from *M. tuberculosis* were lower than the melting temperature of stearic acid (69.6 °C), despite the presence of a hexacosanoyl chain and a long meromycolate chain in the molecule. The enthalpies of fusion of MAs were also unexpectedly small, about a half of the calculated melting enthalpy. The estimated enthalpy of fusion of normal paraffin hydrocarbons, which corresponds to the enthalpy of *trans-gauche* transition of

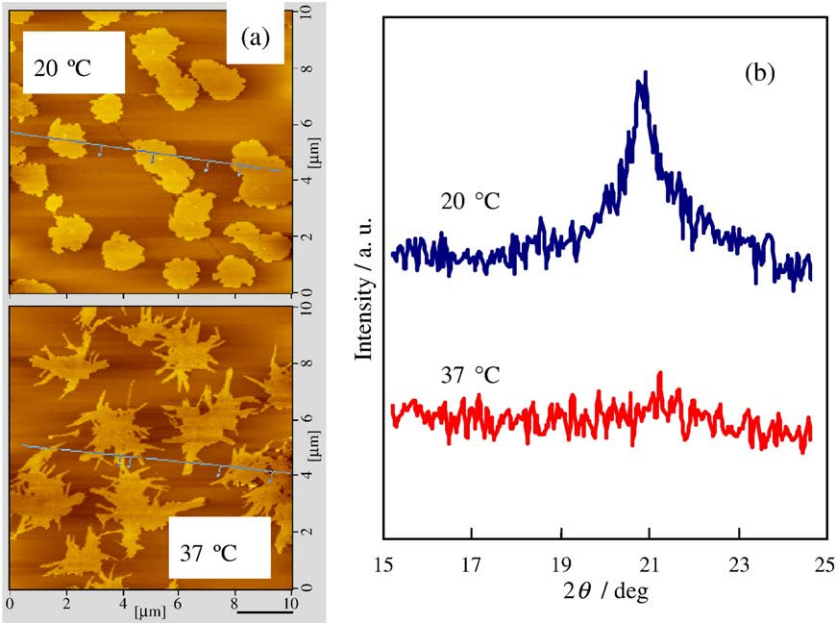

Fig. 5. (a) AFM images of single layered LB film of α-MA prepared at 20 °C (top) and at 37 °C. Bar=2 µm. (b) In-plane XRD patterns of 19 monolayered LB film of α-MA at 20 and 37 °C.

the alkyl chains and disordering the molecules, is ca. 3 kJ/(mole CH_2 [19]). Again, the intra-chain functional groups hinder the all-*trans* conformation of the meromycolate chain, thus causing poor packing of the hydrophobic chains.

3.2. Fine structures of LB films

Figs. 5a and b demonstrate the AFM images and the in-plane XRD patterns, respectively, of the LB films of α-MA. Those films were prepared by depositing the water-surface monolayer of α-MA onto a solid substrate at temperatures 20 °C and 37 °C at $\pi = 25$ mN m^{-1}. The topography at 20 °C is clearly different from that at 37 °C, and the difference may correspond to the presence of different LC phases in the Langmuir monolayers of α-MA at $\pi = 25$ mN m^{-1}, as demonstrated in the phase diagram (Fig. 3a). Round domains of areas 2–5 μm^2 are seen in the film prepared at 20 °C whereas slightly shrunk ones with prickles are in the film prepared at 37 °C.

The in-plane XRD pattern at 20 °C shows a single diffraction peak at $2\theta = 21°$ due to the isotropic hexagonal spacing of 4.2 Å, which is not noted in the diagram of the film deposited at 37 °C. The E value for the LC phase in the Langmuir monolayer above 37 °C was shown to be about 150 mN m^{-1}, some 50 mN m^{-1} smaller than the E value for the LC phase below 29 °C, which was about 200 mN m^{-1}. The LC phase at above 37 °C is probably less orderly than the one at temperatures below 29 °C. The results of the in-plane XRD measurements performed on the MeO-MA and the Keto-MA LB films are shown in Figs. 6a and b, respectively. The diffraction pattern of the MeO-MA LB film at 20 °C gave a single peak and the one at 37 °C, none. In the case of Keto-MA, the films prepared at 20 °C and 37 °C both gave an analogous peak. These observations agree with their phase behavior: The Langmuir monolayer of MeO-MA at $\pi = 25$ mN m^{-1} was in the LC phase at 20 °C, and in the LE phase at 37 °C, whereas the Keto-MA monolayer at $\pi = 25$ mN m^{-1} was in the LC phase at both temperatures.

The present results from the LB film studies might not be directly applied to the Langmuir monolayer, as the LB films or monolayers transferred onto a solid substrate may not have the same structural features as the original monolayer at the air/water interface. However, the present LB films were prepared under the same conditions excepting for the transfer temperature. Thus, we can safely attribute the difference observed between the two LB films by AFM or XRD to the difference in the structures of the phases formed at 20 and 37 °C and $\pi = 25$ mN m^{-1}.

3.3. Possible conformations of MAs at air/water interface

Figs. 7a–c show the average molecular areas at the film collapse point A^{cp} and those at the phase transition point A^{tr} at various temperatures of α-MA, MeO-MA and Keto-MA, respectively. Careful analysis of these diagrams may give information about the possible conformation of the MA molecules in the Langmuir monolayers. Clear differences are seen between the three diagrams. In the case of α-MA monolayer, A^{cp} may be as small as 50 $Å^2$ $molecule^{-1}$ and the largest A^{cp} is 63 $Å^2$ $molecule^{-1}$. In the Ket-MA monolayer, A cannot take a smaller value than 80 $Å^2$ $molecule^{-1}$. Since the Keto-MA monolayer is in the SC phase at π^{cp}, it suggests that in each molecule in the monolayer, four hydrocarbon chains are tightly packed. The carbonyl group in the meromycolate chain is hydrated at the air/water interface to give a W-shaped conformation with four hydrocarbon chains packing together in parallel to the Keto-MA molecule.

This four-chain folding of Keto-MA also offers an explanation for the presence of a methyl branch adjacent to keto and other MA oxygen functions. Keto fatty acids have melting points slightly higher than those of their straight-chain analogues, as exemplified by 12-oxooctadecanoic (m.p. 79–80 °C) and octadecanoic (m.p. 69–70 °C)

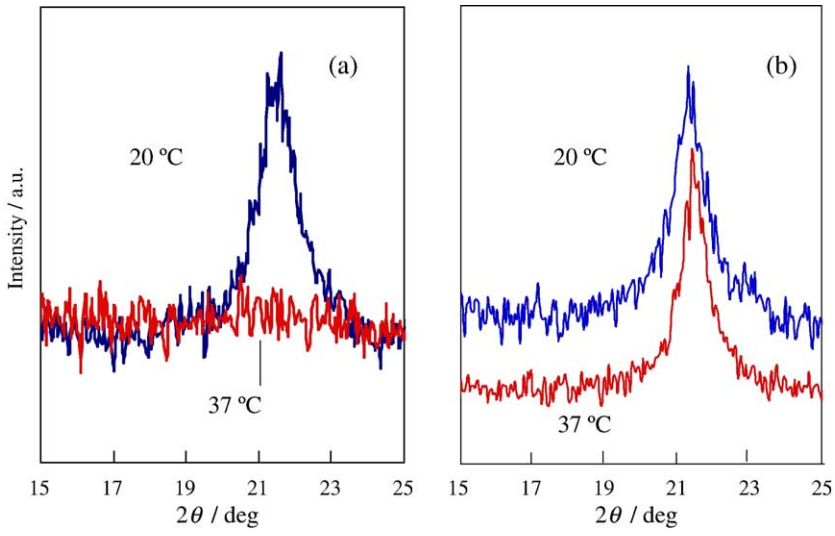

Fig. 6. In-plane XRD patterns of 19 monolayered LB films prepared at 20 and 37 °C: (a) MeO-MA; (b) Ket-MA.

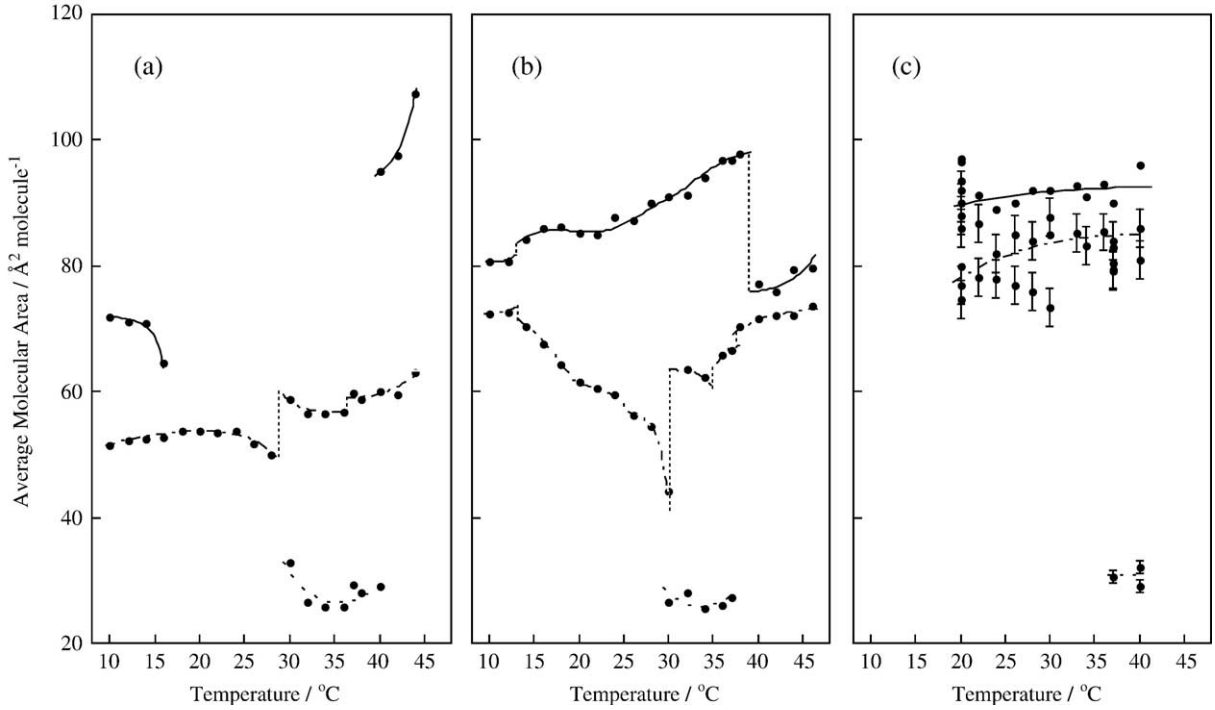

Fig. 7. Average molecular areas at phase transition pressures A^{tr} at various temperatures T (—) and average molecular areas at the collapse pressures A^{cp} at various T (•—•—•). Molecular areas at unresolved transition pressures at various T (- - - -) is also included when obtained. (a) α-MA; (b) MeO-MA; (c) Keto-MA.

acids. Similarly, 9-octadecanone (m.p. 44–45 °C) melts at higher temperature than octadecane (m.p. 28–30 °C) but 10-methyl-9-octadecanone [20] is a liquid at room temperature. These latter data clearly indicate that introduction of a methyl branch adjacent to a keto group may introduce a degree of flexibility sufficient to allow molecular folding.

In the case of MeO-MA, A^{tr} varies from 81 to 98 Å^2 molecule^{-1} and A^{cp} from 44 to 73 Å^2 molecule^{-1}. It is considered that the methoxy group in the meromycolate chain is weakly hydrophilic so that at low surface pressure and low T, it may be hydrated to stabilize a W-shaped conformation (81 Å^2 molecule^{-1}). However at higher surface pressure and/or higher T, the methoxy group may detach from the water surface, thereby allowing the molecules to take more compact form. and then resulting in Van der Waals interaction, which is energetically more favorable. This suggestion is supported by the fact that π^{tr} decreases as T increases. The detaching process and changing of conformation however are implied to be a very slow process as suggested by the large multiphase regions in Fig. 3b.

In the case of α-MA monolayer, A^{cp} may be as small as 50 Å^2 molecule^{-1} and the largest A^{cp} is 63 Å^2 molecule^{-1}. It needs further analysis to identify the definite conformation of MA molecules in the monolayer, but it is reasonable to assume that MeO-MA and α-MA take more flexible conformation, changeable in accord to various factors including temperature and surface pressure.

The π–A isotherms of α-MA and Keto-MA reported in the work by Hasegawa et al. [15,17] do not quite agree with our results, e.g., the molecular areas at the collapse surface pressure reported are much smaller and the collapse surface pressures much lower than ours. It might partly be due to the different experimental conditions between them and us, especially the concentration of the sample solutions for spreading: the concentration they used was about 14 times that used by us, which might have caused partial crystallization of MAs on the trough water surface after evaporation of the spreading solvent. Another cause could be the difference in the origins (strain) of the samples, which were not specified in their works.

4. Conclusions

The profiles of the π vs. A isotherms of insoluble monolayers of the α-MA, MeO-MA and Keto-MA are significantly temperature dependent and the phase diagrams of the monolayers of the MAs are quite different from each other. The α-MA film includes a wide liquid condensed phase region. The MeO-MA also produces liquid condensed phase, along with a multiphase over a wide range of surface pressure and temperature. Only the Keto-MA forms a solid condensed phase along with the liquid condensed phase.

Each MA film has distinctive A^{tr} and A^{cp} values, suggesting that the optimal conformations are related to the individual features of the functional groups in the meromycolate chain. The carbonyl group of Keto-MA is probably hydrated at the water surface, so that Keto-MA adopts a relatively constrained W-conformation. Since the methoxy group of MeO-MA has some water affinity and cyclopropanes in α-MA no hydrophilicity, those MA are considered to be taking more flexible conformations depending

upon the environmental factors including surface pressure and temperature.

In relating the present results to the biological role of mycolic acids, the most valuable finding is the special behavior of the Keto-MA. It has exceptional rigidity in monolayers, over a wide temperature range (Fig. 4c), apparently assuming a W-shaped conformation with four hydrocarbon chains packing together in parallel. To our knowledge, this is the first time that fatty acid packing of this type has been detected in nature. The initial studies [21,22] on the location of functional groups in cyclopropyl MA showed that these fatty acids are assembled according to a generalized template, with groups spaced at regular intervals separated by relatively uniform lengths of hydrocarbon chains (Table 1); these results have been thoroughly substantiated in recent studies [4,5]. The current results offer the first justification for this exquisite regular architecture of mycobacterial MAs. The true reason for the presence of oxygenated functions in MAs is also revealed as being necessary for conformational stabilization probably through hydrophilic interactions. In this model monolayer study, the hydrophilic interaction is most likely to be with the aqueous sub-phase. In the cell envelope of mycobacteria, however, the interaction of the keto group could either be with the covalently attached arabinogalactan or, more intriguingly, with the mycolic acid 3-hydroxy group. This latter interaction could take place in an inter- or intramolecular fashion.

Biological activities of living cells rely upon, not only the relevant chemical reactions but also on relating physicochemical or physical processes. In this study, we have shown that MAs of different chemical structures form Langmuir monolayers having distinctive physicochemical features and each MA exhibits multiple phase transitions depending upon the temperature and the surface pressure. Dubnau et al. [23] reported that in a *M. tb* strain whose cell wall-linked mycolate consists solely of α-MA, the permeation rate was very low, and Yuan et al. [24] reported that in a recombinant mycobacterial strain whose Keto-MA is completely replaced by MeO-MA showed poor growth in macrophages and a decreased rate of permeation for hydrophilic substances. Those studies imply that different mycolates in the cell envelope contribute differently to the permeability function of the mycolate layer of the cell envelope. It seems possible that each component mycolate takes different conformation in the cell envelope mycolate layer as suggested by the present study, and that the different forms of different mycolates have different effects on the cell function, though we should be careful in applying the monolayer results to the natural cell wall mycolate layer functions.

Acknowledgements

This research was supported partly by Saneyoshi Scholarship Foundation and partly by Innovative Research Organization for the New Century, Saitama University.

References

[1] M. Rouhi, Tuberculosis: a tough adversary, Chem. Eng. News 77 (1999) 52–70.
[2] P.J. Brennan, H. Nikaido, The envelope of mycobacteria, Annu. Rev. Biochem. 64 (1995) 29–63.
[3] P.J. Brennan, Structure, function, and biogenesis of the cell wall of *Mycobacterium tuberculosis*, Tuberculosis 83 (2003) 91–97.
[4] M. Watanabe, Y. Aoyagi, M. Ridell, D.E. Minnikin, Separation and characterization of individual mycolic acids in representative mycobacteria, Microbiology 147 (2001) 1825–1837.
[5] M. Watanabe, Y. Aoyagi, H. Mitome, T. Fujita, H. Naoki, M. Ridell, D.E. Minnikin, Location of functional groups in mycobacterial meromycolate chains; the recognition of new structural principles in mycolic acids, Microbiology 148 (2002) 1881–1902.
[6] D.E. Minnikin, Lipids: complex lipids, their chemistry, biosynthesis and roles, in: C. Ratledge, J. Stanford (Eds.), The Biology of the Mycobacteria, vol. 1, Academic Press, London, England, 1982, pp. 94–184.
[7] D.E. Minnikin, L. Kremer, L.G. Dover, G.S. Besra, The methyl-branched fortifications of *Mycobacterium tuberculosis*, Chem. Biol. 9 (2002) 545–553.
[8] N. Rastogi, Recent observations concerning structure and function relationships in the mycobacterial cell envelope: elaboration of a model in terms of mycobacterial pathogenicity, virulence and drug-resistance, Res. Microbiol. 142 (1991) 464–476.
[9] M. Jackson, C. Raynaud, M.-A. Lanèelle, C. Guilhot, C. Laurent-Winter, D. Ensergueix, B. Gicquel, M. Daffé, Inactivation of the antigen 85C gene profoundly affects the mycolate content and alters the permeability of the *Mycobacterium tuberculosis* cell envelope, Mol. Microbiol. 31 (1999) 1573–1587.
[10] J. Liu, H. Nikaido, A mutant of *Mycobacterium smegmatis* defective in the biosynthesis of mycolic acid synthesis accumulates meromycolates, Proc. Natl. Acad. Sci. U. S. A. 96 (2000) 4011–4016.
[11] H. Nikaido, S.-H. Kim, E.Y. Rosenberg, Physical organization of lipids in the cell wall of *Mycobacterium chelonae*, Mol. Microbiol. 8 (1993) 1025–1030.
[12] X. Hong, A.J. Hopfinger, Construction, molecular modeling, and simulation of *Mycobacterium tuberculosis* cell walls, Biomacromolecules 5 (2004) 1052–1065.
[13] S. Staellberg-Stenhagen, E. Stenhagen, A monolayer and X-ray studies of mycolic acid from the human tubercle bacillus, J. Biol. Chem. 150 (1945) 255–262.
[14] T. Hasegawa, J. Nishijo, M. Watanabe, K. Funayama, T. Imae, Conformational characterization of α-mycolic acid in a monolayer film by the Langmuir–Blodgett technique and atomic force microscopy, Langmuir 16 (2000) 7325–7330.
[15] T. Hasegawa, R.M. Leblanc, Aggregation properties of mycolic acid molecules in monolayer films: a comparative study of compounds from various acid-fast bacterial species, Biochim. Biophys. Acta 1617 (2003) 89–95.
[16] T. Hasegawa, J. Nishijo, M. Watanabe, J. Umemura, Y. Ma, G. Sui, Q. Huo, R.M. Leblanc, Characteristics of long-chain fatty acid monolayers studied by infrared external-reflection spectroscopy, Langmuir 18 (2002) 4758–4764.
[17] T. Hasegawa, S. Amino, S. Kitamura, R. Matsumoto, S. Katada, J. Nishijo, Study of the molecular conformation of α- and keto-mycolic acid monolayers by the Langmuir–Blodgett technique and Fourier transform infrared reflection-adsorption spectroscopy, Langmuir 19 (2003) 105–109.
[18] J.T. Davies, E.K. Rideal, Interfacial Phenomena, Academic Press, New York, 1961, p. 265.
[19] P.J. Flory, A. Vrij, Melting points of linear-chain homologues. The normal paraffin hydrocarbons, J. Am. Chem. Soc. 85 (1963) 3548–3553.
[20] G. Tsuchihashi, K. Tomooka, K. Suzuki, Completely stereospecific 1,2- migration of alkyl groups in diethylaluminum chloride (Et_2AlCl)

promoted pinacol-type rearrangement, Tetrahedron Lett. 25 (1984) 4253–4256.
[21] D.E. Minnikin, N. Polgar, The methoxymycolic and ketomycolic acids from human tubercle bacilli, Chem. Commun. (1967) 916–918.
[22] D.E. Minnikin, N. Polgar, The mycolic acids from human and avian tubercle bacilli, Chem. Commun. (1967) 1172–1174.
[23] E. Dubnau, J. Chan, C. Raynoud, V.P. Mohan, M.-A. Lanèelle, K. Yu, A. Quemard, I. Smith, M. Daffé, Oxygenated mycolic acids are necessary for virulence of *Mycobacterium tuberculosis* in mice, Mol. Microbiol. 36 (2000) 630–637.
[24] Y. Yuan, Y.Q. Zhu, D.D. Crane, C.E. Barry III, The effect of oxygenated mycolic acid composition on cell wall function and macrophage growth in *Mycobacterium tuberculosis*, Mol. Microbiol. 29 (1998) 1449–1458.